ACS Photonics

Letter

pubs.acs.org/journal/apchd5

Hybrid Magnetoplasmonic Crystals Boost the Performance of Nanohole Arrays as Plasmonic Sensors

Blanca Caballero,[†] Antonio García-Martín,[†] and Juan Carlos Cuevas*[,‡]

[†]IMM-Instituto de Microelectrónica de Madrid (CNM-CSIC), Isaac Newton 8, PTM, Tres Cantos, E-28760 Madrid, Spain

[‡]Departamento de Física Teórica de la Materia Condensada and Condensed Matter Physics Center (IFIMAC), Universidad Autónoma de Madrid, E-28049 Madrid, Spain

Supporting Information

ABSTRACT: We present here a theoretical study that shows how the use of hybrid magnetoplasmonic crystals comprising both ferromagnetic and noble metals leads to a large enhancement of the performance of nanohole arrays as plasmonic sensors. In particular, we propose using Au−Co−Au films perforated with a periodic array of subwavelength holes as transducers in magneto-optical surface-plasmon-resonance sensors, where the sensing principle is based on measurements of the transverse magneto-optical Kerr effect. We demonstrate that this detection scheme may result in bulk figures of merit that are 2 orders of magnitude larger than those of any other type of plasmonic sensor. The sensing strategy put forward here can make use of the different advantages of nanohole-based plasmonic sensors such as miniaturization, multiplexing, and its combination with microfluidics.

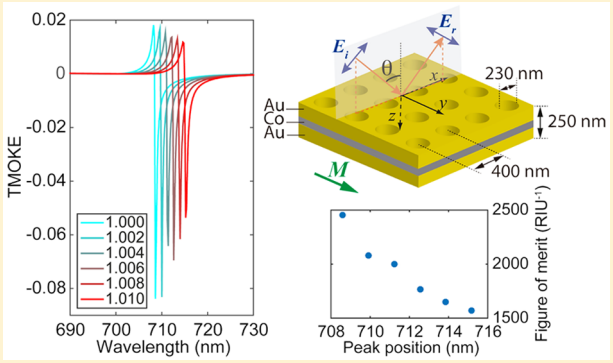

KEYWORDS: *plasmonic sensors, nanohole arrays, magnetoplasmonic crystals, transverse magneto-optical Kerr effect*

Plasmonic structures are widely used in low-cost, label-free biosensors, and the investigation of how to improve their sensitivity or to widen their range of applications is a central topic in the field of plasmonics.[1,2] The most commonly used plasmonic sensors are based on the concept of surface plasmon resonance (SPR) and, in particular, on the sensitivity of these resonances to changes in the refractive index of the medium surrounding a metallic structure.[3,4] These SPR-based sensors are commercially available, and they are able to detect changes on the refractive index of the sensing medium as small as 10^{-7}. In the search for an improved bulk sensitivity of SPR-based sensors, researchers have proposed different strategies. Thus, for instance, it has been shown that the use of the magneto-optical (MO) properties of layered systems containing magnetic materials can, in principle, enhance the sensitivity of these sensors.[5−10] Another possibility that is becoming increasingly popular is the use of nanohole arrays or perforated metallic membranes featuring arrays of subwavelength holes.[11−25] These sensors make use of the extraordinary optical transmission phenomenon,[26,27] which originates from the resonant excitation of surface plasmons in these periodically patterned nanostructures. Nanohole arrays exhibit a series of advantages over conventional SPR-based sensors. First of all, since these periodic systems do not require additional prisms to excite the plasmonic modes, they can be more easily miniaturized and integrated in nanoscale devices. Also, nanohole arrays are compatible with imaging-based devices and can be implemented in a microarray format for multiplexed and high-throughput biosensing.[28] In addition, nanohole arrays can also be combined with microfluidic systems to implement real-time analysis of biomolecular binding kinetics.[15,29] Furthermore, since these perforated membranes are based on metal films, one can use the transducer surface as an electrode to implement additional techniques either for manipulating or for detecting molecules such as electrochemistry, dielectrophoresis, or resistive heating.[24] Finally, the performance and operational parameters (wavelength, refractive index range, etc.) can be further tuned in a straightforward way by, for instance, modifying the geometrical parameters in these arrays (lattice parameter, hole size and shape, membrane thickness, etc.)[30−32] or by engineering the substrate.[25]

In spite of the attractive features of nanohole-based sensors described above, conventional SPR sensors are still the choice for most sensing applications. This is not only due to the fact that nanohole arrays require somehow more sophisticated, and therefore more expensive, fabrication techniques but also due to the fundamental fact that normally nanohole-based sensors do not reach the sensitivity and resolution that is routinely achieved with SPR sensors. This lower spectral resolution is mainly due to larger radiative losses, which immediately translate into broader resonance line widths. Thus, one of the major open problems in the topic of plasmonic sensors is to find novel strategies to considerably boost the resolution of

Received: November 13, 2015
Published: January 19, 2016

DOI: 10.1021/acsphotonics.5b00658
ACS Photonics 2016, 3, 203−208

nanohole arrays as biosensors. In this context, the goal of this work is to show that the performance of nanohole arrays as plasmonic sensors can be dramatically enhanced by using hybrid perforated membranes containing both ferromagnetic and noble metals as the nanohole array transducer (Figure 1).

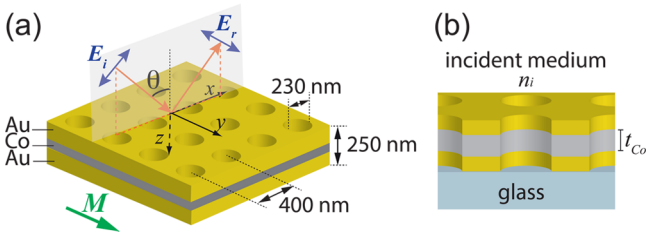

Figure 1. (a) Schematic representation of a Au−Co−Au perforated membrane with a periodic array of circular holes forming a square lattice. We display the values of different geometrical parameters such as the lattice constant, the hole diameter, the membrane total thickness, and the Co thickness, t_{Co}. We also indicate the Co magnetization, M, which is parallel to the plane of the membrane and perpendicular to the incidence plane. (b) Lateral cut of the hybrid membrane that is placed on a glass substrate.

The idea is to make use of the MO properties of these systems in the spirit of MO-SPR sensors,[5−10] rather than measurements of the transmission at normal incidence as in standard nanohole-based sensing experiments. To be precise, we propose to make use of the transverse MO Kerr effect (TMOKE), which consists in the change of the amplitude of reflected p-polarized light when the magnetization of the ferromagnetic layer lies in the plane of the film and is perpendicular to the plane of incidence (Figure 1a). We show here that the TMOKE in these hybrid nanohole arrays is largely enhanced due to the interplay between the MO properties of the ferromagnetic membrane and the excellent plasmonic properties of noble metals, which is a central idea in the emerging field of magnetoplasmonics.[33,34] This interplay leads to extremely sharp Fano-like features in the MO response that, in addition, are very sensitive to changes in the refractive index of the surrounding medium, making these magnetoplasmonic crystals ideal for sensing applications. In fact, as we show below, the corresponding sensing figure of merit of these hybrid systems can be several orders of magnitude larger than that of other plasmonic sensors, including standard nanohole arrays, SPR and MO-SPR sensors, and sensors based on localized surface plasmon resonances.[2,35] We would like to stress that the fabrication of the hybrid magnetoplasmonic crystals that we propose here is clearly feasible with present technology. In fact, nonmagnetic hybrid nanohole arrays of various kinds have already been investigated experimentally,[36,37] including hybrid Au−Fe−Au magnetoplasmonic crystals fabricated by using self-assembled nanosphere lithography.[38] Let us also mention that the fabrication and characterization of cm^2 disordered nanohole arrays based on Au−Co multilayers have been recently reported,[39] using a low-cost fabrication technique that also allows for periodically ordered systems.

RESULTS AND DISCUSSION

In order to demonstrate the central idea of this work, we study a hybrid Au−Co−Au perforated membrane with a periodic array of subwavelength circular holes forming a square lattice (Figure 1a). The Co layer is located in the middle of the structure and has a thickness t_{Co} (Figure 1b). We consider that the substrate is made of glass with a refractive index of 1.5 in the whole explored wavelength range, and the incident medium and the interior of the holes have a refractive index n_i ($n_i = 1$ for air). Throughout this work, we assume that the lattice parameter of the hole array is 400 nm, the hole diameter is 230 nm, and the total thickness of the membrane is 250 nm.

As explained above, the sensing principle is based on the transverse MO Kerr effect. To be precise, the quantity of interest in this case is

$$\mathrm{TMOKE} = \frac{R_{pp}(+M) - R_{pp}(-M)}{R_{pp}(+M) + R_{pp}(-M)} \quad (1)$$

which measures the relative change in the reflection probability for p-polarized light, R_{pp}, upon reversal of the magnetization of the Co layer, M, which is parallel to this layer but perpendicular to the plane of incidence. Notice that this quantity is bounded between −1 and +1, and it does not involve the reflection in the demagnetized state, which is always experimentally troublesome. The TMOKE vanishes at normal incidence, and therefore, it has to be measured at an oblique incidence. Unless otherwise stated, we shall assume that the angle of incidence is $\theta = 45°$ (where it reaches its maximum value in conventional, nonresonant, continuous media) and that the incident light propagates along the x-axis, as indicated in Figure 1a.

In order to compute the TMOKE in these hybrid membranes, we have made use of a generalization of the scattering-matrix approach of Whittaker and Culshaw[40] that we have recently developed.[41] This generalization allows us to describe any magneto-optical effect in periodically patterned multilayer structures, and, to our knowledge, it is the only method that has shown to be capable of computing the TMOKE signal in fully three-dimensional nanostructured media such as our system of study (see Methods for further details). In our calculations, the optical constants of Au were taken from ref 42, while the optical and MO constants of Co were taken from ref 43.

Let us start our analysis with the characterization of the optical and MO properties of the Au−Co−Au nanohole arrays assuming that the incident medium is air ($n_i = 1$). In Figure 2a we show the reflectivity, R_{pp}, for a demagnetized sample ($M = 0$) as a function of the wavelength and for different values of the Co thickness t_{Co}. We focus here on the wavelength range between 690 and 730 nm, which is where the important action takes place for our choice of geometrical parameters of the nanohole array. As one can see, the inclusion of Au in this membrane (or the reduction of the Co thickness) leads to the appearance of a pronounced minimum at around 709 nm, where the reflectivity almost vanishes. This minimum is due to the resonant excitation of a surface plasmon that appears at the air−Au interface (see Supporting Information for details). In Figure 2b we display the corresponding change in reflectivity upon reversal of the magnetization, $R_{pp}(+M) - R_{pp}(-M)$. The main feature in this case is the change of sign that appears for many hybrid structures close to the reflectivity minimum. This change of sign stems from the small nonreciprocal variation in the surface plasmon wavevector induced by the magnetization of the Co layer.[33] This variation, which depends on the magnetization direction, shifts the reflectivity curves in opposite directions for different signs of M, which leads to a sign change in the difference $R_{pp}(+M) - R_{pp}(-M)$. Finally, we show in Figure 2c the corresponding results for the TMOKE, as defined

DOI: 10.1021/acsphotonics.5b00658
ACS Photonics 2016, 3, 203−208

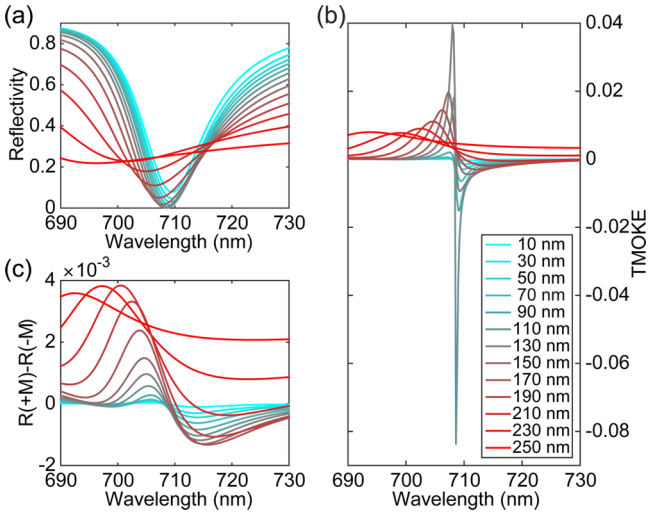

Figure 2. (a) Computed reflectivity, R_{PP}, for a Au−Co−Au nanohole array where the Co layer is demagnetized ($M = 0$) as a function of the wavelength of the incident light. The different curves correspond to different values of the Co thickness, t_{Co}, as indicated in the legend of panel (c). (b) Corresponding change in reflectivity upon reversal of the Co magnetization. (c) Corresponding TMOKE, as defined in eq 1.

in eq 1, which is our quantity of interest. As one can see, depending on the Co thickness, the TMOKE can adopt very large values accompanied by a change of sign close to the wavelength of the reflectivity minimum, exhibiting very sharp Fano-like line shapes. This line shape is especially sharp for a Co thickness t_{Co} = 110 nm, which is the value that we shall consider from now on.

Let us turn now to the central issue of this work, namely, the use of these hybrid nanohole arrays for sensing applications. To illustrate this, we have studied how the TMOKE of the hybrid membrane with t_{Co} = 110 nm is modified upon changing the refractive index of both the incident medium and the interior of the holes, n_i, presenting the results in Figure 3a. This analysis corresponds to what is referred to as a flow-over sensing

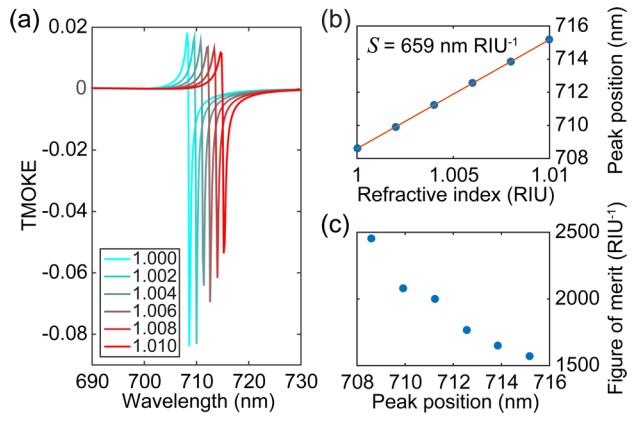

Figure 3. (a) TMOKE of a Au−Co−Au nanohole array with a Co thickness of 110 nm as a function of the wavelength of the incident light for different values of the refractive index of the incident medium, n_i, which is assumed to be the same as that of the holes. (b) Position of the Fano-like feature as a function of n_i. The blue symbols correspond to the results of panel (a), and the red solid line corresponds to a fit to a straight line, whose slope defines the bulk sensitivity of our device, $S = \Delta\lambda/\Delta n_i$ = 659 nm/RIU. (c) Corresponding figure of merit as a function of wavelength; see text for definition.

scheme,[23] where the substrate is not modified during the sensing procedure. From the results shown in Figure 3a, one can see that the position of the Fano-like feature in the TMOKE curves is very sensitive to variations in n_i and is red-shifted as n_i increases. This red shift is simply due to a change in the resonant condition of the surface plasmon excitation, which depends on the refractive index n_i (see Supporting Information). To quantify the sensing performance, we follow the usual practice and define the bulk refractive index sensitivity as $S = \Delta\lambda/\Delta n_i$, where $\Delta\lambda$ is the shift of the Fano-like feature and Δn_i is the change in the refractive index of the incident medium. As we show in Figure 3b, the sensitivity of our hybrid nanohole sensor is 659 nm/RIU. Since the actual accuracy in the tracking of the Fano-like feature also depends on its line width, the most relevant parameter defining the performance of this kind of devices is the figure of merit (FoM), obtained by dividing the bulk sensitivity S by the width of the Fano-like feature Γ, i.e., FoM = S/Γ. This quantity is widely accepted as a proper measure for the performance of plasmonic biosensors based on surface and localized plasmon resonances.[2,20,35,44,45] To obtain Γ in an accurate manner, we fitted the TMOKE line shapes as a function of the wavelength, λ, to a Fano line shape of the form[20]

$$\mathrm{TMOKE}(\lambda) = A + B\frac{(q\Gamma/2 + \lambda - \lambda_0)^2}{(\Gamma/2)^2 + (\lambda - \lambda_0)^2} \quad (2)$$

where Γ describes the line width, λ_0 is the resonant wavelength that defines the position of the Fano-like feature, q is the Fano parameter, and A and B are constants describing the background and the overall peak height, respectively. The details of the fits of the experimental curves can be found in the Supporting Information. With these definitions, the extracted FoMs for our hybrid device reach huge values up to several thousands $(\mathrm{RIU})^{-1}$, as we show in Figure 3c.

To put these numbers into perspective, let us first recall that conventional SPR-based sensors made of gold films using the Kretschmann configuration have a theoretical upper FoM limit of around 108 $(\mathrm{RIU})^{-1}$,[46] which is more than an order of magnitude smaller than the FoM of our hybrid nanohole arrays. In the context of nanohole-based sensors, let us mention that a very recent work based on high-quality Au nanohole arrays with engineered substrates has reported a similar bulk sensitivity of 671 nm/RIU, but a much smaller FoM of 42 $(\mathrm{RIU})^{-1}$ in a similar wavelength range.[25] To our knowledge, the record FoM in nanohole-based sensors is around 162, and it was obtained using the extraordinary light transmission phenomenon through high-quality-factor subradiant dark modes.[20] Thus, we see that our proposal can indeed lead to an improvement of the record for the FoM by more than an order of magnitude. On the other hand, recent advances in plasmonic sensing that make use of localized SPRs have boosted their performance, and FoMs of about 100−150 $(\mathrm{RIU})^{-1}$ have been recently reported,[35,45] which are still much smaller than the values found here. To further illustrate the high performance of our proposal, we have also compared our hybrid nanohole arrays with a successful realization of an MO-SPR-based sensor, which has been shown to be superior to standard SPR sensors.[8] This sensor comprises a Au−Co−Au planar trilayer made of thin films (15 nm Au/6 nm Co/25 nm Au), it makes use of the Kretschmann configuration, and it utilizes the TMOKE as a sensing signal, in the same spirit as in our hybrid nanohole arrays. In Figure 4 we show a comparison of the TMOKE

DOI: 10.1021/acsphotonics.5b00658
ACS Photonics 2016, 3, 203−208

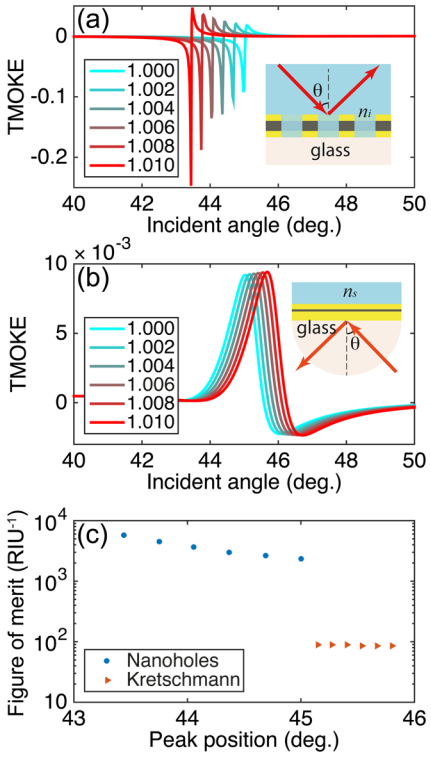

Figure 4. (a) TMOKE of a Au−Co−Au nanohole array with a Co thickness of 110 nm as a function of the angle of incidence and for a wavelength of 709 nm. The different curves correspond to different values of the refractive index of the incident medium. (b) The same as in panel (a) computed for a Au−Co−Au planar trilayer (15 nm Au/6 nm Co/25 nm Au) in the Kretschmann configuration and for a wavelength of 632 nm.[8] The prism in this scheme is a glass of refractive index equal to 1.5, and what is varied in this case is the refractive index of the substrate, n_s. The inset shows a schematic representation of this MO-SPR sensor. (c) Comparison of the respective figures of merit of the sensors of panels (a) and (b).

signals and FoMs computed for both types of sensors. In this case, and following the usual practice in MO-SPR sensors, we have calculated the TMOKE as a function of the angle of incidence and for a fixed wavelength (709 nm for the nanoholes and 632 nm for the planar thin film trilayer, for which this MO-SPR sensor was optimized). Notice also that in this sensing scheme the TMOKE of the hybrid nanohole arrays exhibits Fano-like line shapes that are very well suited for sensing purposes. In particular, we have used eq 2 to fit the TMOKE line shapes in Figure 4a,b, replacing the wavelength by the angle of incidence. As we summarize in Figure 4c, the performance of our hybrid perforated membranes is again much better than in this MO-SPR sensor, reaching huge FoMs of up to 6000, which are more than 50 times larger than in conventional SPR-based sensors. Such FoM values would result in a substantial improvement of the detection limit of nanohole-based sensors that, in turn, should enable the discrimination of biomolecules with similar refractive indexes that are not possible to differentiate with conventional sensors.

It is fair to point out that our proposal certainly complicates the sensing setups. Apart from the additional difficulties in the fabrication method, the measurement of the TMOKE requires the incorporation of a magnet. However, we think that the tremendous improvement in the performance of the sensors clearly compensates those eventual disadvantages. In this respect, it is worth remarking that there is still plenty of room for improving the results reported here by modifying, for instance, the lattice parameters, hole shapes and sizes, or membrane thickness or by engineering the substrate. In order to illustrate this idea, we show in the Supporting Information that impressive figures of merit larger than 10^4 can be achieved with nanohole arrays with a triangular lattice, a type of lattice that can be realized with low-cost self-assembled nanosphere lithography.[38]

In summary, we have put forward a new strategy for plasmonic sensing based on the use of hybrid magneto-plasmonic crystals and their MO properties. In particular, we have shown that the combination of the use of Au−Co−Au nanohole arrays with measurements of the transverse MO Kerr effect can lead to a tremendous enhancement of the figure of merit of this type of plasmonic sensors. This idea may resolve the central problem of nanohole-based sensors, and it may also make them the natural choice for a wide variety of applications in the near future.

METHODS

All the calculations presented in this work have been carried out with a generalization of the scattering-matrix approach of Whittaker and Culshaw[40] that we have recently developed.[41] This approach combines the scattering-matrix method with the Bloch theorem to describe both the optical and MO properties of arbitrary periodically patterned multilayer structures. In particular, this method is able to deal with MO configurations such as the one realized in the transverse MO Kerr effect, which is out of the scope of other scattering-matrix approaches. Moreover, our method makes use of the so-called fast Fourier factorization, which allows us to converge the results very accurately upon increasing the number of plane waves used in the calculations. This fact is crucial in cases where there is a high contrast in the dielectric functions of the different materials, as it is the case in our Au−Co−Au membranes. Let us emphasize that all the quantities shown in this work were converged to an accuracy better than 1% (relative error).

ASSOCIATED CONTENT

Supporting Information

The Supporting Information is available free of charge on the ACS Publications website at DOI: 10.1021/acsphotonics.5b00658.

Dispersion relation of the Bragg surface phonon polaritons, TMOKE fits to Fano line shapes, and results for a nanohole array with a triangular lattice (PDF)

AUTHOR INFORMATION

Corresponding Author

*E-mail: juancarlos.cuevas@uam.es.

Notes

The authors declare no competing financial interest.

ACKNOWLEDGMENTS

We thank Alvaro Blanco for insightful comments and for a critical reading of the manuscript. This work has been financially supported by the Spanish Ministry of Economy and Competitiveness (Contract Nos. MAT2011-29194-C02-01, MAT2014-58860-P, FIS2011-28851-C02-01, and FIS2014-53488-P) and by the Comunidad de Madrid (Contract No. S2013/MIT-2740).

DOI: 10.1021/acsphotonics.5b00658
ACS Photonics 2016, 3, 203−208

REFERENCES

(1) Tokel, O.; Inci, F.; Demirci, U. Advances in plasmonic technologies for point of care applications. *Chem. Rev.* **2014**, *114*, 5728−5752.

(2) Estevez, M.-C.; Otte, M. A.; Sepulveda, B.; Lechuga, L. M. Trends and challenges of refractometric nanoplasmonics biosensors: A review. *Anal. Chim. Acta* **2014**, *806*, 55−73.

(3) Raether, H. *Surface Plasmons on Smooth and Rough Surfaces and on Gratings*, Vol. *111*; Springer-Verlag: Berlin, 1988.

(4) Maier, S. A. *Plasmonics: Fundamentals and Applications*, 1st ed.; Springer: New York, 2007.

(5) Sepúlveda, B.; Calle, A.; Lechuga, L. M.; Armelles, G. Highly sensitive detection of biomolecules with the magneto-optic surface-plasmon-resonance sensor. *Opt. Lett.* **2006**, *31*, 1085−1087.

(6) Regatos, D.; Fariña, D.; Calle, A.; Cebollada, A.; Sepúlveda, B.; Armelles, G.; Lechuga, L. M. Au/Fe/Au multilayer transducers for magneto-optic surface plasmon resonance sensing. *J. Appl. Phys.* **2010**, *108*, 054502.

(7) Regatos, D.; Sepúlveda, B.; Fariña, D.; Carrascosa, L. G.; Lechuga, L. M. Suitable combination of noble/ferromagnetic metal multilayers for enhanced magneto-plasmonic biosensing. *Opt. Express* **2011**, *19*, 8336−8346.

(8) Manera, M. G.; Montagna, G.; Ferreiro-Vila, E.; González-García, L.; Sánchez-Valencia, J. R.; González-Elipe, A. R.; Cebollada, A.; Garcia-Martin, J. M.; Garcia-Martin, A.; Armelles, G.; Rella, R. Enhanced gas sensing performance of TiO_2 functionalized magneto-optical SPR sensors. *J. Mater. Chem.* **2011**, *21*, 16049−16056.

(9) Manera, M. G.; Ferreiro-Vila, E.; Cebollada, A.; García-Martín, J. M.; García-Martín, A.; Giancane, G.; Valli, L.; Rella, R. Ethane-bridged Zn porphyrins dimers in Langmuir-Schäfer thin films: Spectroscopic, morphologic, and magneto-optical surface plasmon resonance characterization. *J. Phys. Chem. C* **2012**, *116*, 10734−10742.

(10) Manera, M. G.; Ferreiro-Vila, E.; Garcia-Martin, J. M.; Garcia-Martin, A.; Rella, R. Enhanced antibody recognition with a magneto-optic surface plasmon resonance (MO-SPR) sensor. *Biosens. Bioelectron.* **2014**, *58*, 114−120.

(11) Brolo, A. G.; Gordon, R.; Leathem, B.; Kavanagh, K. L. Surface plasmon sensor based on the enhanced light transmission through arrays of nanoholes in gold films. *Langmuir* **2004**, *20*, 4813−4815.

(12) De Leebeeck, A.; Kumar, L. K. S.; de Lange, V.; Sinton, D.; Gordon, R.; Brolo, A. G. On-chip surface-based detection with nanohole arrays. *Anal. Chem.* **2007**, *79*, 4094−4100.

(13) Schatz, G. C.; McMahon, J. M.; Gray, S. K. Tailoring the parameters of nanohole arrays in gold films for sensing applications. *Proc. SPIE* **2007**, *6641*, 664103.

(14) Gordon, R.; Sinton, D.; Kavanagh, K. L.; Brolo, A. G. A new generation of sensors based on extraordinary optical transmission. *Acc. Chem. Res.* **2008**, *41*, 1049−1057.

(15) Eftekhari, F.; Escobedo, C.; Ferreira, J.; Duan, X.; Girotto, E. M.; Brolo, A. G.; Gordon, R.; Sinton, D. Nanoholes as nanochannels: Flow-through plasmonic sensing. *Anal. Chem.* **2009**, *81*, 4308−4311.

(16) Artar, A.; Yanik, A. A.; Altug, H. Fabry-Perot nanocavities in multilayered crystals for enhanced biosensing. *Appl. Phys. Lett.* **2009**, *95*, 051105.

(17) Masson, J.-F.; Murray-Methot, M.-P.; Live, L. S. Nanohole arrays in chemical analysis: manufacturing methods and applications. *Analyst* **2010**, *135*, 1483−1489.

(18) Yanik, A. A.; Kamohara, O.; Artar, A.; Geisbert, T. W.; Connor, J. H.; Altug, H. An optofluidic nanoplasmonic biosensor for direct detection of live viruses from biological media. *Nano Lett.* **2010**, *10*, 4962−4969.

(19) Yanik, A. A.; Huang, M.; Artar, A.; Chang, T. Y.; Altug, H. Integrated nanoplasmonic-nanofluidic biosensors with targeted delivery of analytes. *Appl. Phys. Lett.* **2010**, *96*, 021101.

(20) Yanik, A. A.; Cetin, A. E.; Huang, M.; Artar, A.; Mousavi, S. H.; Khanikaev, A.; Connor, J. H.; Shvets, G.; Altug, H. Seeing protein monolayers with naked eye through plasmonic Fano resonances. *Proc. Natl. Acad. Sci. U. S. A.* **2011**, *108*, 11784−11789.

(21) Blanchard-Dionne, A. P.; Guyot, L.; Patskovsky, S.; Gordon, R.; Meunier, M. Intensity based surface plasmon resonance sensor using a nanohole rectangular array. *Opt. Express* **2011**, *19*, 15041−15046.

(22) Huang, M.; Galarreta, B. C.; Cetin, A. E.; Altug, H. Actively transporting virus like analytes with optofluidics for rapid and ultrasensitive biodetection. *Lab Chip* **2013**, *13*, 4841−4847.

(23) Escobedo, C. On-chip nanohole array based sensing: a review. *Lab Chip* **2013**, *13*, 2445−2463.

(24) Dahlin, A. B. Sensing applications based on plasmonics nanopores: The hole story. *Analyst* **2015**, *140*, 4748−4759.

(25) Cetin, A. E.; Etezadi, D.; Galarreta, B. C.; Busson, M. P.; Eksioglu, Y.; Altug, H. Plasmonic nanohole arrays on a robust hybrid substrate for highly sensitive label-free biosensing. *ACS Photonics* **2015**, *2*, 1167−1174.

(26) Ebbesen, T. W.; Lezec, H. J.; Ghaemi, H. F.; Thio, T.; Wolff, P. A. Extraordinary optical transmission through sub-wavelength hole arrays. *Nature* **1998**, *391*, 667−669.

(27) Garcia-Vidal, F. J.; Ebbesen, T. W.; Kuipers, L. Light passing through subwavelength apertures. *Rev. Mod. Phys.* **2010**, *82*, 729−787.

(28) Chang, T. Y.; Huang, M.; Yanik, A. A.; Tsai, H. Y.; Shi, P.; Aksu, S.; Yanik, M. F.; Altug, H. Large-scale plasmonic microarrays for label-free high-throughput screening. *Lab Chip* **2011**, *11*, 3596−3602.

(29) Escobedo, C.; Brolo, A. G.; Gordon, R.; Sinton, D. Optofluidic concentration: Plasmonic nanostructure as concentrator and sensor. *Nano Lett.* **2012**, *12*, 1592−1596.

(30) Lesuffleur, A.; Kumar, L. K. S.; Brolo, A. G.; Kavanagh, K. L.; Gordon, R. Apex-enhanced Raman spectroscopy using double-hole arrays in a gold film. *J. Phys. Chem. C* **2007**, *111*, 2347−2350.

(31) Ctistis, G.; Patoka, P.; Wang, X.; Kempa, K.; Giersig, M. Optical transmission through hexagonal arrays of subwavelength holes in thin metal films. *Nano Lett.* **2007**, *7*, 2926−2930.

(32) Gwinner, M. C.; Koroknay, E.; Fu, L.; Patoka, P.; Kandulski, W.; Giersig, M.; Giessen, H. Periodic large-area metallic split-ring resonator metamaterial fabrication based on shadow nanosphere lithography. *Small* **2009**, *5*, 400−406.

(33) Armelles, G.; Cebollada, A.; García-Martín, A.; González, M. U. Magnetoplasmonics: Combining magnetic and plasmonic functionalities. *Adv. Opt. Mater.* **2013**, *1*, 10.

(34) Caballero, B.; García-Martín, A.; Cuevas, J. C. Faraday effect in hybrid magneto-plasmonic photonic crystals. *Opt. Express* **2015**, *23*, 22238−22249.

(35) Maccaferri, N.; Gregorczyk, K.; de Oliveira, T. V. A. G.; Kataja, M.; van Dijken, S.; Pirzadeh, Z.; Dmitriev, A.; Åkerman, J.; Knez, M.; Vavassori, P. Ultrasensitive and label-free molecular-level detection enabled by light phase control in magnetoplasmonic nanoantennas. *Nat. Commun.* **2015**, *6*, 6150.

(36) Ikenoya, Y.; Susa, M.; Shi, J.; Nakamura, Y.; Dahlin, A. B.; Sannomiya, T. Optical resonances in short-range ordered nanoholes in ultrathin aluminum/aluminum nitride multilayers. *J. Phys. Chem. C* **2013**, *117*, 6373−6382.

(37) Dahlin, A. B.; Mapar, M.; Xiong, K. L.; Mazzotta, F.; Hook, F.; Sannomiya, T. Plasmonic nanopores in metal-insulator-metal films. *Adv. Opt. Mater.* **2014**, *2*, 556−564.

(38) Patoka, P.; Skeren, T.; Higendorff, M.; Zhi, L.; Paudel, T.; Kempa, K.; Giersig, M. Transmission of light through magnetic nanocavities. *Small* **2011**, *7*, 3096−3100.

(39) Armelles, G.; Caballero, B.; Cebollada, A.; Garcia-Martin, A.; Meneses-Rodríguez, D. Magnetic field modification of optical magnetic dipoles. *Nano Lett.* **2015**, *15*, 2045−2049.

(40) Whittaker, D.; Culshaw, I. Scattering-matrix treatment of patterned multilayer photonic structures. *Phys. Rev. B: Condens. Matter Mater. Phys.* **1999**, *60*, 2610−2618.

(41) Caballero, B.; García-Martín, A.; Cuevas, J. C. Generalized scattering-matrix approach for magneto-optics in periodically patterned multilayer systems. *Phys. Rev. B: Condens. Matter Mater. Phys.* **2012**, *85*, 245103.

(42) Johnson, P. B.; Christy, R. W. Optical constants of the noble metals. *Phys. Rev. B* **1972**, *6*, 4370−4379.

DOI: 10.1021/acsphotonics.5b00658
ACS Photonics 2016, 3, 203−208

(43) Ferreiro-Vila, E.; González-Díaz, J.; Fermento, R.; González, M.; García-Martín, A.; García-Martín, J. M.; Cebollada, A.; Armelles, G.; Meneses-Rodríguez, D.; Sandoval, E. Intertwined magneto-optical and plasmonic effects in Ag/Co/Ag layered structures. *Phys. Rev. B: Condens. Matter Mater. Phys.* **2009**, *80*, 125132.
(44) Otte, M. A.; Sepúlveda, B.; Ni, W.; Pérez Juste, J.; Liz-Marzán, L. M.; Lechuga, L. M. Identification of the optimal spectral region for plasmonic and nanoplasmonic sensing. *ACS Nano* **2010**, *4*, 349−357.
(45) Shen, Y.; Zhou, J.; Liu, T.; Tao, Y.; Jiang, R.; Liu, M.; Xiao, G.; Zhu, J.; Zhou, Z.-K.; Wang, X.; Jin, C.; Wang, J. Plasmonic gold mushroom arrays with refractive index sensing figures of merit approaching the theoretical limit. *Nat. Commun.* **2013**, *4*, 2381.
(46) Homola, J., Ed. *Surface Plasmon Resonance Based Sensors*; Springer: New York, 2006.

DOI: 10.1021/acsphotonics.5b00658
ACS Photonics 2016, 3, 203−208